

# A Design Study of A Magnetron Injection Gun for A Gyrotron Oscillator

By

Toshinori MICHISHITA\*, Hiroshi NISHIHARA\*  
and Hiroshi KUBO\*\*

(Received June 22, 1983)

## Abstract

A magnetron injection gun has been designed for an X-band gyrotron oscillator. The design is based on two-dimensional numerical analyses of the equi-potential surfaces and the electron trajectories. The gun can produce a helical beam of electrons with large perpendicular velocities to the magnetic field. The positional velocity spread of the emitting electrons remains within 12% just before injection into an open resonator. The variation of the velocities along the trajectory is studied and compared with that predicted by the adiabatic approximation. The approximation may yield an appreciable deviation due to the neglect of the inward drift of electrons. Typical parameters of the designed electron gun are presented.

## 1. Introduction

Gyrotrons are intense microwave generators. The guns used for them should produce helical electron beams which resonate with the cavity modes via the cyclotron effect. The electrons emitted from the gun increase their velocities perpendicular to the magnetic field due to the adiabatic compression until injected into the cavity. The adiabatic approximation, however, is less valid near the electrodes, due to the inhomogeneity of the electric field<sup>1)</sup>. This results in an inward drift of the electrons and leads the perpendicular velocity to remain relatively low. As a result, the efficiency of the transformation of the beam energy to the microwave energy becomes low.

The gun system, therefore, has to be designed on the basis of a detailed analysis of the electron motion in a proper electric field, which itself is to be optimized simultaneously.

This paper describes a design study of a magnetron injection gun for an X-band gyrotron oscillator. For the purpose of a practical construction, a gun with large

---

\* Department of Nuclear Engineering

\*\* College of General Education

inclined surfaces of the electrodes will be designed. This allows us to easily construct a cathode with a large radius and with a relatively short length. Further, it can reduce the undesirable effect of the beam space charge, since it reduces the density of the emitter current for a given beam intensity. Such electrodes are designed by using the method of conformal mapping<sup>2)</sup>. The motion of electrons is determined by using the relativistic equations of motion in the above optimized electric field and the prescribed magnetic field<sup>3)</sup>. The space charge effect is neglected, since the density is sufficiently small for the considered beam current.

In the following section, the basic equations are given. The gun under consideration will be utilized for an X-band gyrotron. The cathode radius is much larger than the width of the gap between the cathode and the anode, as well as that of the emitting region. It is, therefore, sufficient to deal with the gun system as a two-dimensional system.

In Section 3, results and discussion are given. The final section is devoted to a summary.

## 2. Equations for Calculations

We first consider an electric field in such electrodes as shown in Fig. 1. The wedge-shaped type electrodes usually produce an inhomogeneous electric field between them. In a two dimensional system, the fields can be easily determined by the conformal mapping method. Then, the electric field are given by

$$E_x = G_1 E_{x0} + G_2 E_{y0}, \quad (1)$$

$$E_y = G_1 E_{y0} - G_2 E_{x0}; \quad (2)$$

$$E_{x0, y0} = \frac{U_0}{r_0} \cdot \frac{\exp[-\pi x/4r_0]}{A} \cdot \left(\frac{A \pm B}{2}\right)^{1/2}, \quad (3)$$

$$A = \{\exp[\pi x/r_0] - 2\cos(\pi y/r_0) + \exp[-\pi x/r_0]\}^{1/2}, \quad (4)$$

$$B = \exp[\pi x/2r_0] \cdot \cos(y/r_0) - \exp[-\pi x/2r_0], \quad (5)$$

$$G_{1,2} = Re, Im\{[x-a] + i(y-h)]^{-1/(1+k_1)}\} \\ \times [(x-b) + iy]^{1/(1+k_2)}, \quad (6)$$

where  $U_0$  is the potential,  $r_0$  is the anode radius,  $a$  and  $b$  are the 'bent' points of the anode and cathode, respectively, with respect to the coordinate  $x$ , and  $h$  is the bent point with respect to  $y$ . The equi-potential surfaces are solved in order to determine the desired configuration of the electrodes. The surfaces are determined

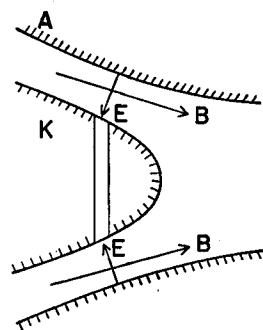


Fig. 1. Magnetron injection gun system.  $E$  and  $B$  are the electric and magnetic fields respectively. The hatched region represents the electrodes of the anode (A) and the cathode (K).

by solving the equation

$$\frac{dy}{dx} = -\frac{E_x}{E_y}. \quad (7)$$

The integration scheme employed is the Runge-Kutta-Gill method for solving Eq. (7).

The magnetic field is given, based on the field profile produced by available air-core solenoid coils. The field along the axis,  $B(x)$ , can be represented by the superposition of fields with Lorentzian forms and is given by

$$B(x) = B_0 \sum \frac{\alpha_i}{1 + \{(x - c_i)/d_i\}^2}, \quad (8)$$

where  $B_0$  is the maximum of the field;  $c_i$  is the coordinate of the maximum on the axis for each field component, and  $d_i$  its half-width. Only one side of the maximum of  $B(x)$  is needed to describe the magnetic field for the calculation of the trajectories. From the analytic continuity, we can find the components of  $B(x)$ . As a result, we have

$$B_x(x, y) = B_0 \sum_i \frac{\alpha_i \left\{ 1 + \left( \frac{x - c_i}{d_i} \right)^2 - \left( \frac{y}{d_i} \right)^2 \right\}}{1 + \left\{ \left( \frac{x - c_i}{d_i} \right)^2 - \left( \frac{y}{d_i} \right)^2 \right\}^2 + 4 \left( \frac{x - c_i}{d_i} \right)^2 \left( \frac{y}{d_i} \right)^2}, \quad (9)$$

$$B_y(x, y) = B_0 \sum_i \frac{\alpha_i \cdot 2 \cdot i \cdot \left( \frac{x - c_i}{d_i} \right) \left( \frac{y}{d_i} \right)}{1 + \left\{ \left( \frac{x - c_i}{d_i} \right)^2 - \left( \frac{y}{d_i} \right)^2 \right\}^2 + 4 \left( \frac{x - c_i}{d_i} \right)^2 \left( \frac{y}{d_i} \right)^2}. \quad (10)$$

In the fields of  $\mathbf{E}$  and  $\mathbf{B}$  given by Eqs. (1), (2), (9) and (10), the trajectories of the electrons are determined from the relativistic equations of motion in the following form;

$$\frac{d\mathbf{v}}{dt} = \eta \gamma^{-1} \left[ \mathbf{E} + \mathbf{v} \times \mathbf{B} - (\mathbf{v} \cdot \mathbf{E}) \frac{\mathbf{v}}{c^2} \right], \quad (11)$$

$$\frac{d\mathbf{r}}{dt} = \mathbf{v}, \quad (12)$$

where  $c$  is the light speed,  $\gamma = [1 - v^2/c^2]^{-1/2}$  the relativistic factor, and  $\eta$  the charge-to-mass ratio. In the calculation, the system is written for a positive charged particle for the numerical convenience.

For the numerical calculation, the variables are transformed into

$$\begin{aligned} \xi_i &= r_i/r_0, \quad \zeta_i = v_i/\sqrt{2\eta U_0}, \quad c_0 = c/\sqrt{2\eta U_0}, \\ \hat{E}_i &= E_i r_0 \sqrt{2U_0}, \quad \hat{B}_i = B_i r_0 / \sqrt{2\eta U_0}, \quad \tau = t \sqrt{2\eta U_0} / r_0, \end{aligned} \quad (13)$$

where  $i = x, y$ , and  $z$ . After these transformations, Eqs. (11) and (12) become

$$\frac{d\zeta_x}{d\tau} = \gamma^{-1}[\hat{E}_x - \zeta_x \hat{B}_y - (\zeta_x \hat{E}_x + \zeta_y \hat{E}_y) \zeta_x / c_0^2], \quad (14)$$

$$\frac{d\zeta_y}{d\tau} = \gamma^{-1}[\hat{E}_y + \zeta_x \hat{B}_x - (\zeta_x \hat{E}_x + \zeta_y \hat{E}_y) \zeta_y / c_0^2], \quad (15)$$

$$\frac{d\zeta_z}{d\tau} = \gamma^{-1}[\zeta_x \hat{B}_y - \zeta_y \hat{B}_x - (\zeta_x \hat{E}_x + \zeta_y \hat{E}_y) \zeta_z / c_0^2], \quad (16)$$

$$\frac{d\xi_i}{d\tau} = \zeta_i, \quad i=x, y, \text{ and } z. \quad (17)$$

Equations (14) – (17) are numerically solved by the standard two-sided Runge-Kutta-Gill method with a FACOM 200 computer in Kyoto University.

### 3. Results

Figure 2 shows the equi-potential surfaces for the values of  $a = -0.3$ ,  $b = 0$ ,  $k_1 = 5$ ,  $k_2 = 4$ , and  $h = 1.4$ . The electrodes are designed along the surfaces, which correspond to the fat solid curves in Fig. 2. In this case, the electrode surfaces have a large angle of  $\theta = 32.2^\circ$  to the axis of the system. We see that the equi-potentials are rather inhomogeneous, especially near the electrodes. Such inhomogeneity plays an important role for the electron trajectories.

In order to couple the beam with cavity modes effectively, we have to make an injection of the beam into a cavity at a proper radial position. For the  $TE_{01}$  mode, for example, the injected radial position has to be  $0.48r_w$  at which the azimuthal electric field of the mode is maximum, where  $r_w$  is the radius of the cylindrical cavity.

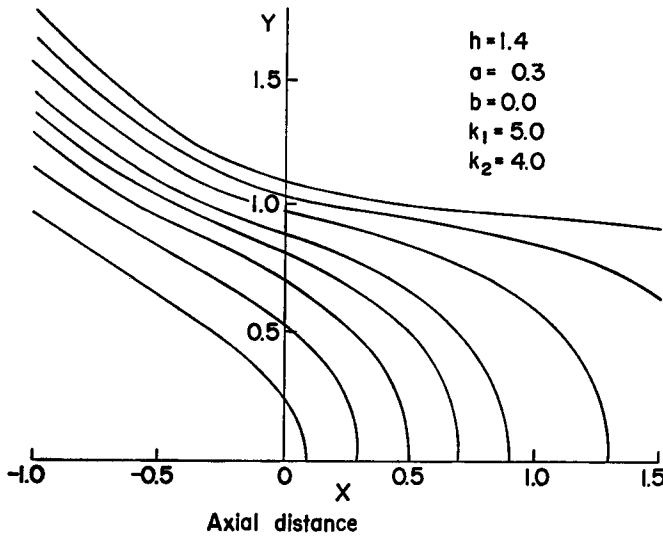


Fig. 2. Equipotential lines for design of the electrodes. Parameters are  $h = 1.4$ ,  $a = 0.3$ ,  $b = 0$ ,  $k_1 = 5$ , and  $k_2 = 4$ .

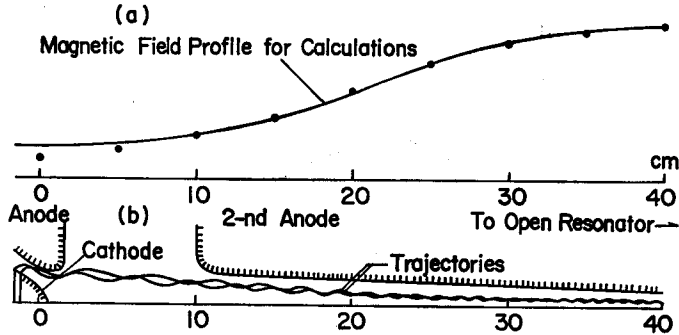


Fig. 3. (a) : Profile of magnetic field intensity along the axis of the system. (b) : Typical trajectories of the emitted electrons until they are injected into an open resonator.

Figure 3 shows a typical case of electron trajectories in such a magnetic field as is shown in Fig. 3(a). The magnetic field corresponds to the case of  $\alpha_1=0.9$ ,  $c_1=20$ ,  $d_1=7.5$ ,  $\alpha_2=0.3$ ,  $c_2=13$ ,  $d_2=5$ ,  $\alpha_3=0.1$ ,  $c_3=-5$ , and  $d_3=5$ , where the last three represent a field produced by a coil set near the gun.

In Fig. 3(b), we see that the trajectories do not intersect with each other until the first return near the electrodes. This will reduce an undesirable effect resulting from the intersection, *i.e.* a significant increase in the space charge. After leaving the cathode, the electrons gradually drift inward with the Larmor motion. The electron beam is injected into the cavity at the radial position  $r_b=0.24r_k$ , where  $r_k$  is the cathode radius at the emitting region. In this case, the radius of the cavity should be chosen as  $r_w=2.08 r_b$  for effectively coupling with the  $TE_{01}$  mode. Note that in the adiabatic approximation we have  $r_b=(B_k/B_0)^{1/2}r_k$  at the injection position. This yields  $r_b=0.45r_k$  for the present value of  $B_k/B_0=1/5$ , which is larger than that in the numerical result. The reason is that we have neglected the inward drift in the adiabatic approximation. Thus, the adiabatic approximation becomes less valid for describing the motion of the electrons in the rather inhomogeneous field. This is more clearly seen in the variation of velocities.

Figure 4 shows a typical case of the electron energy,  $\gamma-1$ , the velocity perpendicular to the magnetic field  $\beta_{\perp}$ , and the velocity parallel,  $\beta_{\parallel}$ , along the trajectory as is shown in Fig. 3(b). In Fig. 4, we see that  $\beta_{\parallel}$  increases almost monotonically, while  $\beta_{\perp}$  oscillates appreciably near the electrodes. This is caused by the difference of the electric field along the Larmor motion. In the very first return of the motion, the electron reaches its own peak of the potential, and then its kinetic energy decreases due to the return to the cathode. A small dip in  $\gamma-1$  corresponds to the return. After being sufficiently apart from the electrodes,  $\beta_{\perp}$  increases, compensating for the decrease in  $\beta_{\parallel}$  according to the adiabatic compression. The ratio of  $\beta_{\perp}$  to  $\beta_{\parallel}$  becomes

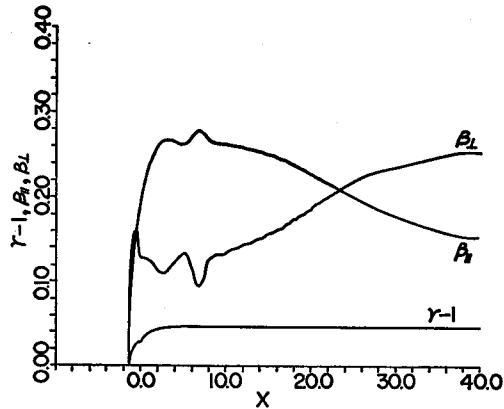


Fig. 4. Variation of the kinetic energy of the electron,  $\gamma-1$ , the perpendicular and parallel velocities,  $\beta_{\perp}$  and  $\beta_{\parallel}$ , respectively, along the trajectory (a) shown in Fig. 3.

1.66 just before being injected into the cavity. The ratio itself depends on the electric field intensity in the present gun system.

Figure 5 shows a typical case of the velocities perpendicular and parallel to the axis,  $\beta_y$  and  $\beta_x$ , respectively. In Fig. 5, we see that  $\beta_y$  exhibits an oscillation superposed with the drift motion near the electrodes. Sufficiently apart from them,  $\beta_y$  exhibits a pure oscillatory motion with an increase of its amplitude. On the other hand,  $\beta_x$  gradually becomes a non-oscillatory motion with a decreased its amplitude.

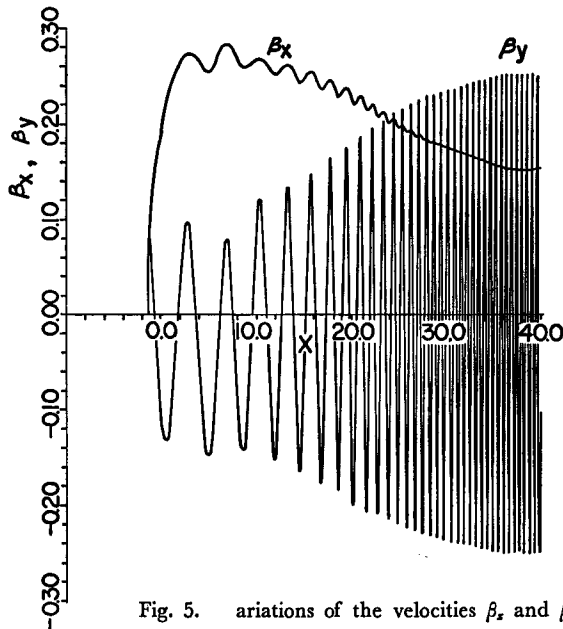


Fig. 5. Variations of the velocities  $\beta_x$  and  $\beta_y$ .

Table : Designed Parameters

Beam Voltage (kV)	20
Average Transverse Velocity ( $v_T/c$ )	0.14
Velocity Ratio $v_L/v_T$	1.5
Velocity Spread of $v_T$ (%)	12
Cathode Radius (mm)	19
Magnetic Field (kG)	3.1
Cyclotron Frequency (GHz)	8.7
Magnetic Field at Cathode (kG)	0.62
Magnetic Compression Ratio	5

#### 4. Summary

We have studied the gun system by solving numerically the relativistic equations of motion in the electrostatic and magnetic fields. It is shown that the perpendicular velocity of the electrons emitted oscillates, and is accompanied by an inward drift near the electrodes. It becomes pure oscillatory just before being injected into the cavity. In the gun system, the adiabatic approximation is less valid with respect to the velocity as well as the trajectory. The gun designed can produce a helical beam of the electrons with a large perpendicular velocity, typically with  $\beta_L/\beta_T \geq 1.5$ .

In the Table, we give the designed parameters typical of the gun. Experiments on a gyrotron utilizing the gun will be separately reported.

#### Acknowledgement

The authors wish to acknowledge their gratitude to Drs. S. Nakamura and T. Yuyama for their fruitful discussions. They also wish to thank Prof. M. Takeyama for his interest.

#### References

- 1) V.K. Lygin and Sh. E. Timring ; Sov. Phys.-Tech. Phys. 16 1316 (1972) ; ibid 16 1809 (1972) ; ibid 18 1067 (1974)
- 2) I. Imai, 'Conformal Mapping and Its Applications', Iwanami Press. Tokyo (1980)
- 3) L. Landau and E. Lifshits, 'Field Theory', Moskaw (1948)